Weierstraß-Institut
für Angewandte Analysis und Stochastik

im Forschungsverbund Berlin e.V.

Preprint ISSN 0946 – 8633

Bifurcations in a model of monolithic passively mode-locked semiconductor laser

Andrei Vladimirov [1], Alexander Pimenov[2], Dmitry Rachinskii [2]

submitted: 17th June 2008

[1] Weierstrass Institute for Applied Analysis and Stochastics
Mohrenstrasse 39
D - 10117 Berlin
Germany
E-Mail: vladimir@wias-berlin.de

[2] Department of Applied Mathematics
University College Cork
Cork, Ireland

E-mail: d.rachinskii@ucc.ie

No. 1334
Berlin 2008

2000 *Mathematics Subject Classification.* 78A60,34C23.

Key words and phrases. semiconductor laser, bifurcations, mode-locking.

1999 *Physics and Astronomy Classification Scheme.* 42.60.Fc 42.55.Px 42.60.Mi 42.65.Pc.

Edited by
Weierstraß-Institut für Angewandte Analysis und Stochastik (WIAS)
Mohrenstraße 39
10117 Berlin
Germany

Fax: + 49 30 2044975
E-Mail: preprint@wias-berlin.de
World Wide Web: http://www.wias-berlin.de/

Abstract

Bifurcation mechanisms of the development and break up of different operation regimes in a passively mode-locked monolithic semiconductor laser are studied by solving numerically partial differential equations for amplitudes of two counterpropagating waves and carrier densities in gain and absorber sections. It is shown that harmonic mode-locking regime with two pulses in the cavity can exhibit a period-doubling bifurcation leading to different amplitudes and separations of the pulses. The effect of linewidth enhancement factors in gain and absorber sections on the laser dynamics is discussed.

1 Introduction

Passively mode-locked semiconductor lasers emit short optical pulses with high repetition rates suitable for application in telecommunication networks [1]. The use of these pulses in modern technology implies several important limitations on their characteristics, such as pulse width, repetition frequency, amplitude noise, time jitter, etc [2]. In particular, elimination of pulse amplitude noise, which appears as a result of the so-called Q-switching instability, constitutes an important technological problem [3]. This oscillatory instability responsible for low frequency (a few GHz) amplitude modulation of mode-locked pulse amplitudes and related to the slow recovery of the intracavity gain medium can be significantly suppressed in quantum dot lasers [4, 5]. Apart from Q-switching instability there are other bifurcation mechanisms of the break-up of the fundamental mode-locking regime. These mechanisms can result in the development of various dynamical regimes, such as harmonic mode-locking regimes with higher repetition rates than that of the fundamental mode-locking, irregular pulsations, and a cw regime.

Numerical study of mode-locking in semiconductor lasers is in the focus of many papers (see, for example, the review paper [6] and references therein). However, only a few of them investigate bifurcation mechanisms of stabilization and destabilization of various regimes in mode-locked lasers. In particular, in Refs. [7, 8, 9, 10, 11] nonlinear bifurcations in a passively mode-locked laser were studied with the help of the recently proposed ring laser model which is based on a system of delay differential equations (DDE) and assumes unidirectional operation approximation.

In this paper, we abandon the ring approximation and use a travelling wave model [12, 13] describing the evolution of two counterpropagating waves in a linear laser. On the basis of the results of Refs. [14, 15, 16, 9], an efficient numerical scheme for the solution of the travelling wave equations is constructed. This numerical scheme is used to describe typical bifurcation sequences that take place with the increase of the injection current in the gain section. We show the existence of large bistability and multistability domains and hysteresis between different dynamical regimes in a mode-locked laser. Moreover, under certain conditions, a period doubling bifurcation of the harmonic mode-locked regime is predicted. This bifurcation leads to the co-existence of the pulses with different amplitudes and different time separations in the laser cavity. Finally, we investigate the effect of the linewidth enhancement factors in the gain and absorber sections on the laser dynamics and demonstrate that the amplitude-phase coupling introduced by these factors can lead to a mode-locked regime with a quasiperiodic laser intensity.

2 Model equations

Let us consider a model of a monolithic semiconductor laser consisting of four sections (see Fig. 1): saturable absorber, gain section, phase tuning section which is used to adjust repetition frequency of mode-locked pulses, and a spectral filtering element [2, 3]. Normalized equations describing temporal and spatial evolution of the amplitudes of two counterpropagating waves $E^{\pm}$ and the carrier density N in the gain and absorber sections can be written in the form

$$\frac{\partial E^{\pm}}{dt} \pm \frac{\partial E^{\pm}}{\partial z} = -\frac{\beta}{2} E^{\pm} + \frac{1 - i\alpha}{2} N E^{\pm}, \tag{1}$$

$$\frac{dN}{dt} = N_0 - \gamma N - sN \left(|E^{+}|^2 + |E^{-}|^2 \right), \tag{2}$$

where the coordinate z along the cavity axis is rescaled in such a way that the group velocity in both laser sections is the same and equal to unity, $v = 1$. In Eqs. (1)-(2) the parameter β describes the linear internal losses in semiconductor material, α is the so-called linewidth enhancement factor, s is inversely proportional to the saturation intensity in the corresponding section, γ is the carrier relaxation rate, and N_0 is unsaturated gain (absorption) in the gain (absorber) section. In general case, all these parameters have different values in different sections. Furthermore, the parameter N_0 is positive in the gain section (amplification) and negative in the absorber section (absorption). Below we assume that $E^{\pm}$ are dimensionless and the variable N has the dimension of inverse time. In our calculations we use the following fixed values for the parameters of the laser sections: $\gamma_g^{-1} = 1$ns, $\gamma_q^{-1} = 10$ ps, $\beta_g^{-1} = \beta_q = 10$ ps, $s_g^{-1} = 10$ ps, $s_q = 0.2$ ps, $L_g/v = 6.25$ ps, $L_q/v = 0.625$ ps, $L_p/v = 5.625$ ps, where the subscripts 'g' and 'q' refer to the gain and the absorber sections, respectively; L_g, L_q, and L_p denote the length of the gain, absorber, and passive sections.

Boundary conditions at the left laser facet $z = 0$ can be written in the form

$$E^{+}(t, 0) = \sqrt{\kappa_1} E^{-}(t, 0), \tag{3}$$

where κ_1 describes the reflectivity of the left facet.

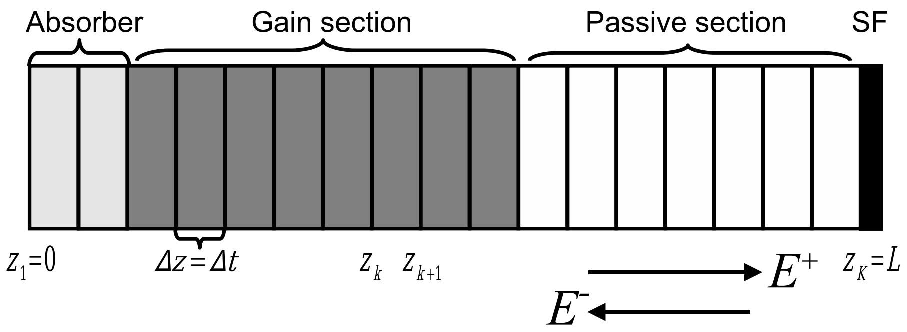

Figure 1: Schematic representation of a monolithic semiconductor laser. The laser sections are split into segments of equal optical length Δz. DBR - distributed Bragg reflection section responsible for the spectral filtering of laser radiation. $E^{\pm}$ – amplitudes of two counterpropagating waves.

Industrial samples of monolithic mode-locked lasers comprise special Bragg reflection sections that act as a spectral filter for laser radiation. In the case when such a section is absent, the spectral filtering results from the finiteness of the spectral bandwidth of the gain section. Here we assume that a thin spectral filtering section is located near the right laser facet. Then the effect of this section on the laser radiation can be described by the following boundary condition:

$$E^{-}(t, L) = \sqrt{\kappa_2} \int_0^{\infty} g(\tau) E^{+}(t-\tau, L), \tag{4}$$

where κ_2 and g describe the reflectivity of the right facet and the form of the spectral filtering profile, respectively. In accordance with [7, 9], we use the Lorentzian shape of the spectral filtering $g(t) = \Gamma \exp(-\Gamma t)$ with the bandwidth Γ. In our calculations we have taken $\kappa_1 = \kappa_2 = 0.3$ and $\Gamma^{-1} = 0.5$ ps.

3 Numerical method

In order to solve Eqs. (1)-(4) we apply a numerical scheme similar to that used in Ref. [15] to study active mode-locking in semiconductor lasers. First, we divide each of the laser sections into a number of segments of equal optical length $\Delta z = \Delta t$ where Δt is the time required for light to pass through this segment (see Fig. 1). Let the total number of segments be K. In each segment $z_k \leq z \leq z_{k+1}$ of the gain and absorber sections we integrate Eqs. (1) for the counterpropagating waves along the characteristics. The solutions are given by

$$E^{+}(t+\Delta z, z_{k+1}) = E^{+}(t, z_k) \exp\left[-\frac{\beta \Delta z}{2} + \frac{1-i\alpha}{2} \int_{z_k}^{z_{k+1}} N(t - z_k + z, z)\, dz\right], \tag{5}$$

$$E^{-}(t+\Delta z, z_k) = E^{-}(t, z_{k+1}) \exp\left[-\frac{\beta \Delta z}{2} + \frac{1-i\alpha}{2} \int_{z_k}^{z_{k+1}} N(t + z_{k+1} - z, z)\, dz\right]. \tag{6}$$

For $\Delta z \ll 1$ the two integrals in Eqs. (5) and (6) can be approximated to the order of Δz^3 by a single time dependent integral

$$G_k(t) = \int_{z_k}^{z_{k+1}} N(t+\Delta z/2, z)\, dz.$$

Using this approximation, we can rewrite the transformations (5) and (6) in the form

$$E^+(t+\Delta z, z_{k+1}) = E^+(t, z_k) \exp\left[-\frac{\beta \Delta z}{2} + \frac{1-i\alpha}{2} G_k(t)\right], \tag{7}$$

$$E^-(t+\Delta z, z_k) = E^-(t, z_{k+1}) \exp\left[-\frac{\beta \Delta z}{2} + \frac{1-i\alpha}{2} G_k(t)\right]. \tag{8}$$

In order to obtain the rate equation for $G_k(t)$, we integrate Eq. (2) over the interval $z_k \leq z \leq z_{k+1}$ and arrive at

$$\begin{aligned} \frac{dG_k}{dt} &= G_0 - \gamma G_k - s\int_{z_k}^{z_{k+1}} N(t+\Delta z/2, z)\, |E^+(t+\Delta z/2, z)|^2 dz \\ &\quad - s\int_{z_k}^{z_{k+1}} N(t+\Delta z/2, z)\, |E^-(t+\Delta z/2, z)|^2 dz, \end{aligned} \tag{9}$$

where $G_0 = N_0 \Delta z$ is the cumulative unsaturated gain (loss) associated with the segment $z_k \leq z \leq z_{k+1}$ of the gain (absorber) section. The integrals in this equation can be approximated as follows. Multiplying Eqs. (1) by the complex conjugate amplitudes $\bar{E}^\pm$ and considering the real part of the resulting equations, we obtain

$$\frac{\partial |E^\pm|^2}{dt} \pm \frac{\partial |E^\pm|^2}{\partial z} = (-\beta + N)\, |E^\pm|^2.$$

Integration of these equations along the characteristics leads to

$$|E^+(t+\Delta z, z_{k+1})|^2 - |E^+(t, z_k)|^2 = \int_{z_k}^{z_{k+1}} (N(t - z_k + z, z) - \beta) |E^+(t - z_k + z, z)|^2 dz, \tag{10}$$

$$|E^-(t+\Delta z, z_k)|^2 - |E^-(t, z_{k+1})|^2 = \int_{z_k}^{z_{k+1}} (N(t + z_{k+1} - z, z) - \beta) |E^-(t + z_{k+1} - z, z)|^2 dz, \tag{11}$$

where at $\beta = 0$ the integrals in the right hand side of (10) and (11) can be up to the order Δz^3 approximated by the two integrals from the right hand side of Eq. (9). Therefore, using relations (7)-(8), (10)-(11) and the trapezoidal approximation to the integrals

$$-\beta \int_{z_k}^{z_{k+1}} |E^-(t + z_{k+1} - z, z)|^2 dz, \qquad -\beta \int_{z_k}^{z_{k+1}} |E^+(t - z_k + z, z)|^2 dz,$$

and assuming that $\beta \Delta z \ll 1$ we obtain

$$\frac{dG_k}{dt} = G_0 - \gamma G_k - s e^{-\beta \Delta z/2} \left(e^{G_k} - 1\right) \left[|E^+(t, z_k)|^2 + |E^-(t, z_{k+1})|^2\right]. \tag{12}$$

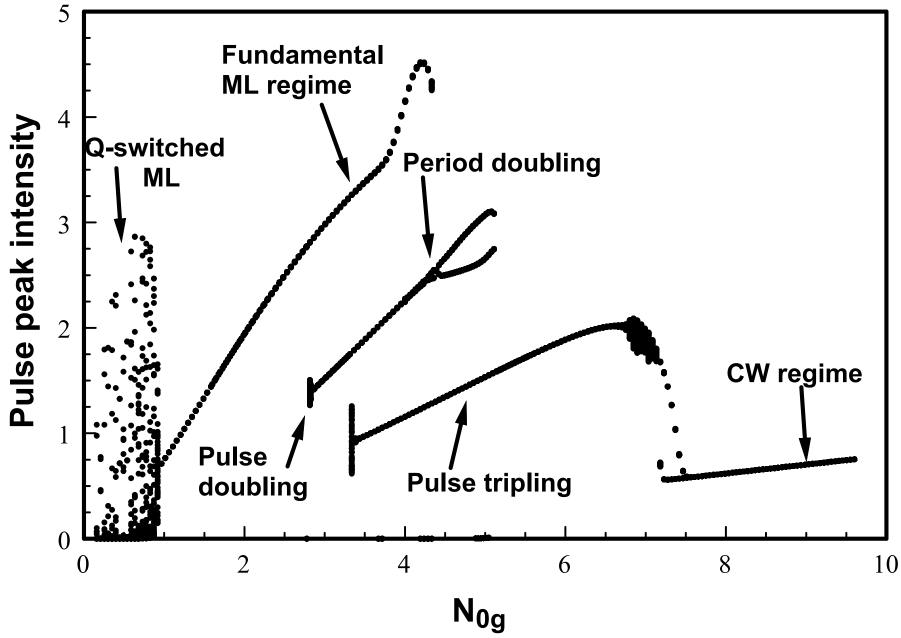

Figure 2: Numerical bifurcation diagram illustrating different operation regimes of a monolithic mode-locked laser. $N_{0q} = -32$, $\alpha_g = \alpha_q = 0$.

The system of coupled differential-algebraic Eqs. (7), (8), (12) approximates the evolution of the electric field envelopes and the carrier density in the gain and absorber sections. To solve these equations we used the time discretization $\Delta t = \Delta z$, consistent with the space discretization, and an implicit numerical scheme for the differential equation (12). To describe the transformation of the amplitudes $E^{\pm}$ in the passive section the algebraic relations (7) and (8) with $G_k = 0$ were used.

4 Bifurcation diagrams

Fig. 2 presents a bifurcation diagram, which was obtained by the numerical solution of Eqs. (7), (8), (12) with the boundary conditions (3) and (4). In this figure local maxima of the intensity time traces of the electric field amplitude $|E^{+}(t, L)|^2$ at the right laser facet are plotted against the value of the control parameter N_{0g} corresponding to the unsaturated gain N_0 in the gain section. The unsaturated loss N_{0q} in the absorber section is fixed for Fig. 2. The sequence of bifurcations shown in this plot is in good qualitative agreement with the results obtained earlier using the DDE mode-locking model [9]. For small injection currents (small N_{0g}) the mode-locking regime is unstable with respect to the Q-switching instability. In the unstable range the amplitude of mode-locked pulses is slowly modulated with the Q-switching frequency $\Omega_Q \approx 3.4$GHz (see Fig. 3). With the increase of the gain current the fundamental mode-locking regime becomes stable. This regime corresponds to a sequence of short pulses with the repetition period close to the cavity round trip time (see Fig. 4a). With further increase of the injection current in the gain section the fundamental mode-locking branch disappears after a saddle-node bifurcation and a sudden jump happens to a harmonic mode-locking regime with approximately the twice higher repetition rate (see Fig. 4b). This regime corresponds to a pair of mode-locked pulses counterpropagating in the cavity. In the framework of the DDE model based on the ring cavity approximation the two pulses are always equidistant and have equal amplitudes (see Ref. [9]). As opposed to this approximation, in a linear laser the branch of harmonic mode-locked pulses can exhibit the period doubling bifurcation leading to different pulse amplitudes and time separations (see Figs. 2 and 4b). This bifurcation has a simple intuitive interpretation. Unlike pulses propagating unidirectionally in a ring laser, the two counterpropagating pulses in a linear cavity must collide in the course of their propagation. If the pulses are identical and are equally spaced in time, the collision takes place in the (optical) midpoint of the cavity. For the parameter values used in our calculations this point is located inside the amplifying medium, not far away from the right end of the gain section. Hence, the collision of two equidistant pulses should result in a strong local saturation in this section which is unfavorable for laser generation. On the other hand, for the regime shown in Fig. 4b with slightly different distances between the two consecutive pulses, only every second collision takes place in the gain section, while the other collisions occur in the phase tuning section. Therefore, the period doubling bifurcation shown in Fig. 2 leads to a reduction of the gain section saturation.

Optical spectra of the fundamental and harmonic mode-locking regimes are presented in the right panel of Fig. 4. For the harmonic mode-locked regime with $M = 3$ pulses co-existing in the cavity only the modes with the numbers $0, \pm M, \pm 2M, ...$ dominate in the spectrum (see Fig. 4c). Due to the period doubling bifurcation leading to different pulse amplitudes and separations, the mode-locked regime with $M = 2$ does not have this property (see Fig. 4b). However, as one could expect, in this regime the modes with the numbers $0, \pm M$ have largest amplitudes in the spectrum. We note that according to the bifurcation diagram shown in Fig. 2 there exist wide ranges in the parameter space where the model equations exhibit bistability and even tristability between different types of mode-locked regimes.

The numerical results presented in Figs. 1, 2, and 4 have been obtained with the zero linewidth enhancement factors $\alpha_{q,q} = 0$ both in the gain and the absorber sections. Fig. 5 presents a diagram similar to that shown in Fig. 2 but obtained by changing simultaneously the linewidth enhancement factors in the gain and absorber sections; the common value $\alpha = \alpha_g = \alpha_q$ of the factors is the bifurcation parameter. One can see that the increase of the α-factors leads to a gradual decrease of the amplitude of the mode-locked pulse and hence to a degradation of the mode-locked regime. Furthermore, at some critical value of the linewidth enhancement factor a sharp transition to a mode-locking regime with an additional small "satellite" pulse following the main pulse takes place (see Fig. 6). The amplitudes of both the pulses are slightly modulated in time, which implies that the regime shown in Fig. 6b corresponds the laser intensity changing quasiperidically in time rather than

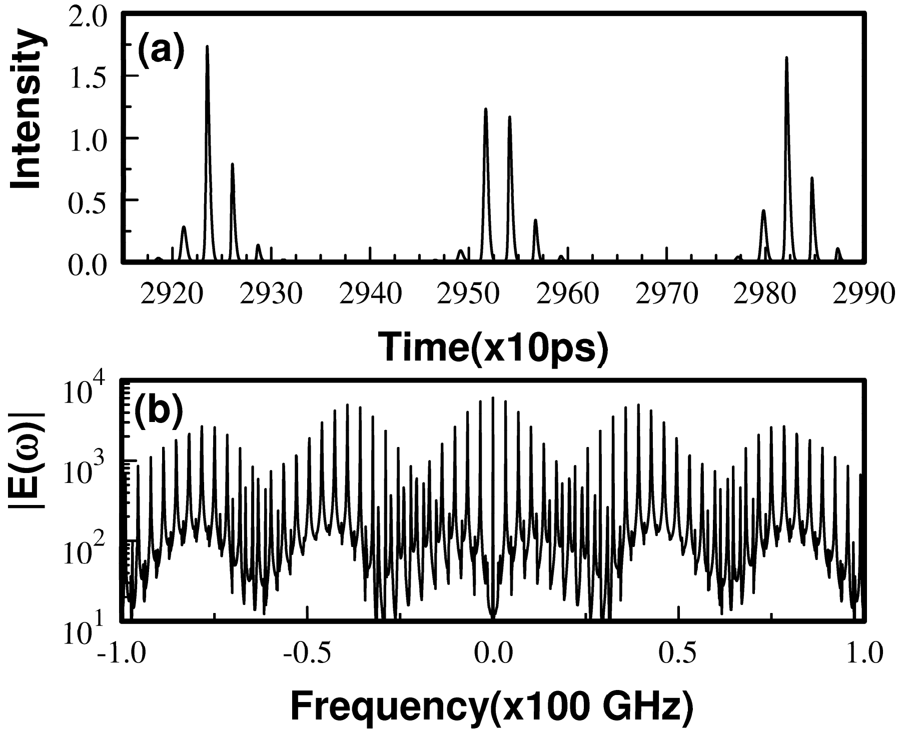

Figure 3: Q-switched ML regime: (a) time trace of the electric field intensity $|E^+(t, L)|^2$; (b) optical spectrum corresponding to the time trace shown in the panel (a). Parameters are the same as in Fig. 2.

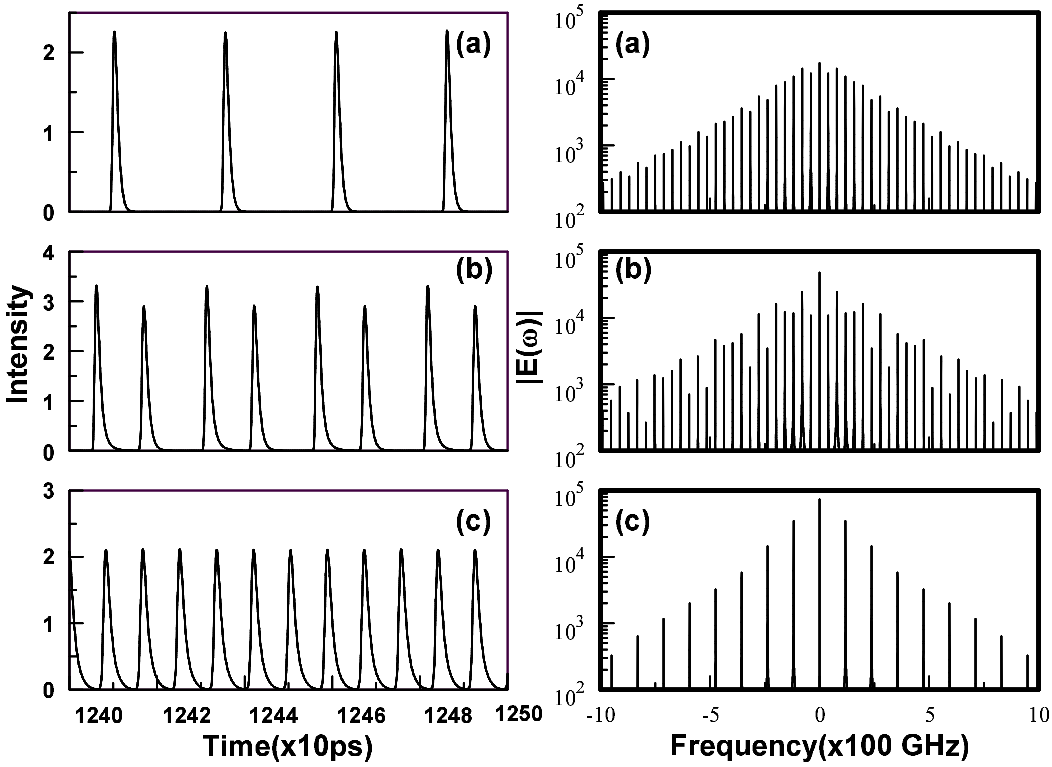

Figure 4: Time traces of the laser intensity $|E^{+}(t, L)|^2$ (left) and the corresponding optical spectra (right): (a) the fundamental ML regime; (b) harmonic ML regime with two pulses in the cavity having different peak power and time separations; (c) harmonic ML regime with three pulses in the cavity. Parameters are the same as in Fig. 2.

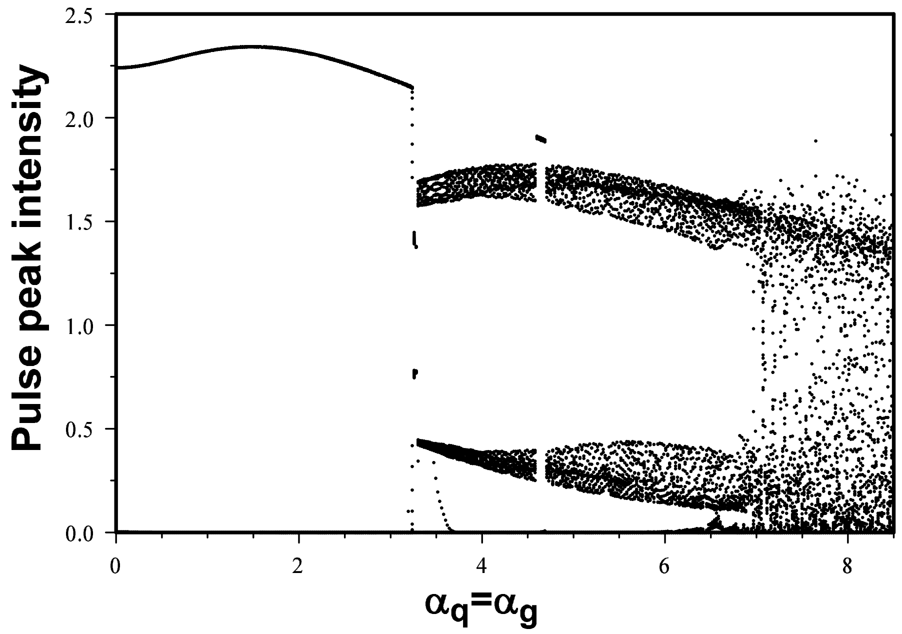

Figure 5: Pulse peak intensity plotted against the varied common value $\alpha = \alpha_g = \alpha_q$ of the linewidth enhancement factors for the gain and absorber sections.

periodically. This is confirmed by the picture of the optical spectrum of this regime shown in the right panel of Fig. 6b, where each of the laser modes is split into two lines with the frequency difference $\Delta\Omega \approx 5.6$GHz, i.e., approximately 7 times smaller than the intermode frequency spacing $\Delta\omega \approx 39.6$ GHz.

The effect of changing the linewidth enhancement factor α_g in the gain section on the fundamental ML regime is illustrated by Fig. 7 obtained for a fixed value of the α factor of the absorber section, which is $\alpha_q = 1$ and $\alpha_q = 3.5$ for Fig. 7a,b, respectively. If follows from this figures that the maximal amplitude of ML pulses is achieved when α-factors of the gain and absorber sections are approximately equal, i.e., $\alpha_g = \alpha_q$, which is in agreement with the result obtained with the DDE model describing a ring laser with unidirectional lasing [9].

5 Conclusions

To study dynamical instabilities in a passively mode-locked semiconductor laser, we have applied an efficient algorithm for numerical analysis of the travelling wave equations describing the space-time evolution of counterpropagating waves in this laser. The results of the numerical implementation of this algorithm appear to be in good qualitative agreement with those obtained with the DDE model describing unidirectional operation in a ring laser. In particular, multistability between the fundamental and different harmonic mode-locking regimes has been demonstrated for wide parameter ranges. However, numerical simulations revealed also certain

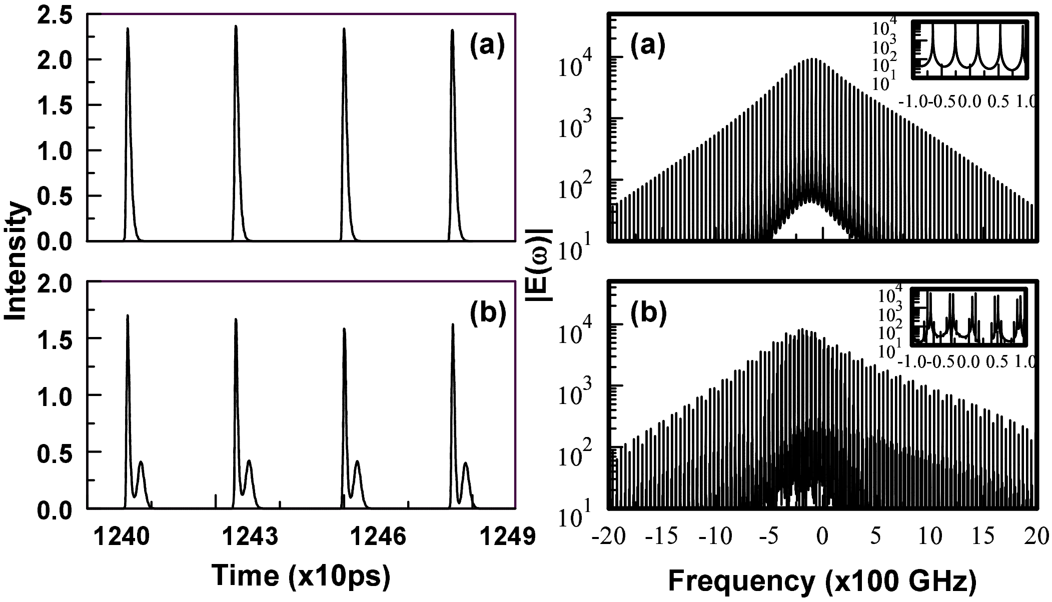

Figure 6: Laser intensity time traces (left) and optical spectra (right) for different mode-locking regimes shown in Fig. 5: (a) The fundamental ML regime for $\alpha_g = \alpha_q = 1$; (b) A quasiperiodic ML regime with a satellite pulse behind the main pulse for $\alpha_g = \alpha_q = 3.5$.

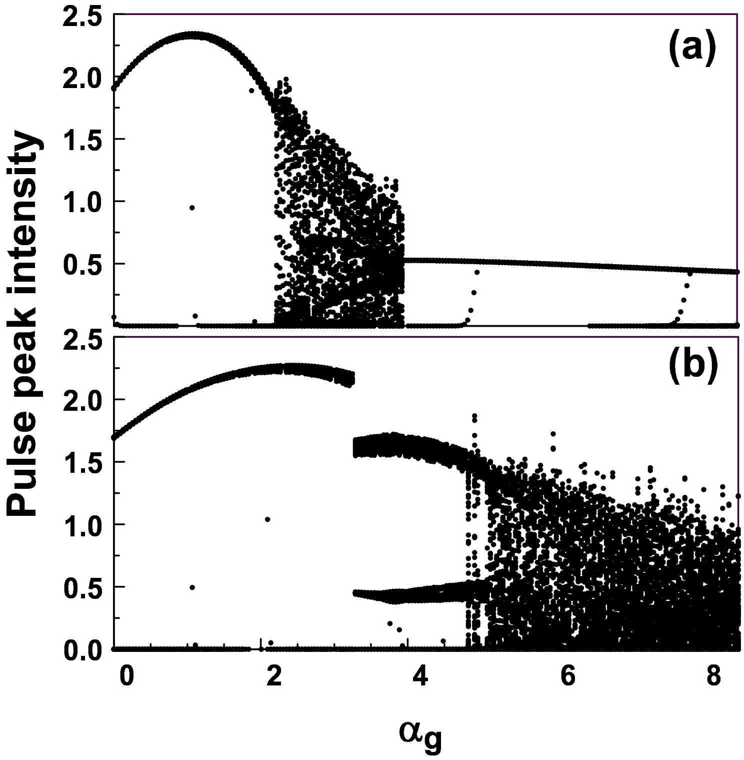

Figure 7: Mode-locking pulse peak intensities for the varied linewidth enhancement factor α_g and fixed α_q: (a) $\alpha_q = 1$; (b) $\alpha_q = 3.5$.

differences between the two models. We have shown that, unlike the ring cavity DDE model, the one based on the travelling wave equations for counterpropagating waves in a linear cavity can exhibit a period doubling bifurcation of the harmonic mode-locked regime with two pulses in the cavity. This bifurcation, resulting in different amplitudes and separations of the two pulses, is related to the increased saturation of the gain section at the point where the counterpropagating pulses collide. We have studied the effect of the α factors in the gain and absorber sections on the dynamics of the mode-locked laser and shown that the maximal intensity of mode-locked pulses is achieved when the α factors in the two sections are approximately equal. A sharp transition to a quasiperiodic mode-locking regime with additional small satellite pulse following the main one is described.

6 Acknowledgments

We are grateful to D. Turaev, M. Radziunas, and M. Wolfrum for useful discussions. This publication has emanated from research conducted with the financial support of Science Foundation Ireland and the project SFB 787 of the DFG.

References

[1] L. A. Jiang, E. P. Ippen, and H. Yokoyama, *Ultrahigh-Speed Optical Transmission Technology* (Springer, 2007), chap. Semiconductor mode-locked lasers as pulse sources for high bit rate data transmission, pp. 21–51.

[2] R. Kaiser and B. Hüttl, IEEE J. Sel. Top. Quantum Electron **13**, 125 (2007).

[3] B. Hüettl, R. Kaiser, C. Kindel, S. Fidorra, W. Rehbein, H. Stolpe, G. Sahin, U. Bandelow, M. Radziunas, A.G.Vladimirov, et al., Appl. Phys. Lett. **88**, 221104 (3 pages) (2006).

[4] Kuntz, G. Fiol, M. Lämmlin, D. Bimberg, M. G. Thompson, K. T. Tan, C. Marinelli, R. V. Penty, I. H. White, V. M. Ustinov, et al., Appl. Phys. Lett. **85**, 843 (2004).

[5] E. Viktorov, P. Mandel, A.G.Vladimirov, and U. Bandelow, Appl. Phys. Lett. **88**, 201102 (3 pages) (2006).

[6] E. Avrutin, J. Marsh, and E. Portnoi, IEE Proc.-Optoelectron. **147**, 251 (2000).

[7] A. Vladimirov, D. Turaev, and G. Kozyreff, Opt. Lett. **29**, 1221 (2004).

[8] A. Vladimirov and D. Turaev, Radiophys. & Quant. Electron. **47**, 857 (2004).

[9] A. Vladimirov and D. Turaev, Phys. Rev. A **72**, 033808 (2005).

[10] D. Rachinskii, A. Vladimirov, U. Bandelow, B. Hüttl, and R. Kaiser, J. Opt. Soc. Am. B **23**, 663 (2006).

[11] M. Nizette, D. Rachinskii, A.G.Vladimirov, and M. Wolfrum, Physica D **218**, 95 (2006).

[12] J. E. Caroll, J. E. A. Whiteaway, and R. G. S. Plumb, *Distributed feedback semiconductor lasers* (IEE, 1998).

[13] U. Bandelow, M. Radziunas, J. Sieber, and M. Wolfrum, IEEE J. Quantum Electron. **37**, 2001 (2001).

[14] A. J. Lowery, Proc. IEE **135**, 126 (1988).

[15] R. J. Helkey, P. A. Morton, and J. E. Bowers, Opt. Lett. **15**, 112 (1990).

[16] V. B. Khalfin, J. M. Arnold, and J. H. Marsh, IEEE J. Sel. Top. Quantum Electron. **1**, 523 (1995).